



Biochar as a sustainable electrode material for electricity production in microbial fuel cells



Tyler Huggins^a, Heming Wang^a, Joshua Kearns^a, Peter Jenkins^b, Zhiyong Jason Ren^{a,*}

^a Department of Civil, Environmental, and Architectural Engineering, University of Colorado, Boulder, Boulder, CO 80309, United States

^b Department of Mechanical Engineering, University of Colorado, Denver, CO 80204, United States

HIGHLIGHTS

- Biochar can be a new and sustainable material for microbial fuel cell electrodes.
- Biochar MFCs showed comparable performance to activated carbon and graphite granule.
- Biochar has economical and environmental benefits compared to other materials.

ARTICLE INFO

Article history:

Received 15 November 2013

Received in revised form 13 January 2014

Accepted 15 January 2014

Available online 24 January 2014

Keywords:

Biochar
Electrode
Microbial fuel cell
Bioelectrochemical
Electricity

ABSTRACT

Wood-based biochars were used as microbial fuel cell electrodes to significantly reduce cost and carbon footprint. The biochar was made using forestry residue (BCc) and compressed milling residue (BCp). Side-by-side comparison show the specific area of BCp ($469.9 \text{ m}^2 \text{ g}^{-1}$) and BCc ($428.6 \text{ cm}^2 \text{ g}^{-1}$) is lower than granular activated carbon (GAC) ($1247.8 \text{ m}^2 \text{ g}^{-1}$) but higher than graphite granule (GG) ($0.44 \text{ m}^2 \text{ g}^{-1}$). Both biochars showed power outputs of $532 \pm 18 \text{ mW m}^{-2}$ (BCp) and $457 \pm 20 \text{ mW m}^{-2}$ (BCc), comparable with GAC ($674 \pm 10 \text{ mW m}^{-2}$) and GG ($566 \pm 5 \text{ mW m}^{-2}$). However, lower material expenses made their power output cost $17\text{--}35 \text{ US\$ W}^{-1}$, 90% cheaper than GAC ($402 \text{ US\$ W}^{-1}$) or GG ($392 \text{ US\$ W}^{-1}$). Biochar from waste also reduced the energy and carbon footprint associated with electrode manufacturing and the disposal of which could have additional agronomic benefits.

© 2014 Elsevier Ltd. All rights reserved.

1. Introduction

Microbial fuel cell (MFC) is a new platform technology that can simultaneously achieve organic and inorganic biodegradation and electricity generation (Logan et al., 2006; Wang and Ren, 2013). MFC reactors utilize the metabolic activity of exoelectrogenic bacteria to catalyze redox reactions on the anode and promote the flow of electrons from the anode to the cathode for direct current harvesting (Logan, 2008). One of the most promising applications of MFCs is for wastewater treatment. Compared to current energy and cost intensive treatment processes, several studies calculated and demonstrated that MFCs may result in positive energy output while reducing sludge production by more than 60% (Huggins et al., 2013). MFCs have also been shown to produce biochemicals, disinfectants, as well as the removal of nutrients and metals during the treatment process (Wang and Ren, 2013). However, one key factor that limits the implementation of larger scale MFC systems

is the high cost and non-renewable nature of current electrode materials. For example, several studies estimated that the electrode material may contribute to 20–50% of the overall MFC cost (Rabaey et al., 2010; Rozendal et al., 2009).

Electrodes play a fundamental role in facilitating exoelectrogenic biofilm growth and electrochemical reactions and are essential in improving the functionality and efficiency of MFCs. Ideal electrode materials should possess high surface area, high conductivity, low cost, stability, and biocompatibility. Most electrode materials used in MFCs are carbon based granular activated carbon (GAC) or graphite granules (GGs), especially in large scale systems, because GAC has a high degree of micro-porosity and catalytic activities, and GGs are less expensive with higher conductivity, even though the internal surface area is lower (Wei et al., 2011). The costs of GAC or GG electrodes vary greatly, but on average range from 500 to 2500 US\$ ton⁻¹, which is significantly lower than carbon cloth or carbon paper (100,000–500,000 US\$ m⁻²), but is still considered high for large scale applications. In addition to cost, the life-cycle impact of these materials can be significant depending on feedstock choice and manufacturing. For example,

* Corresponding author. Tel.: +1 (303) 492 4137; fax: +1 (303) 492 7317.

E-mail address: jason.ren@colorado.edu (Z.J. Ren).

GAC is most commonly manufactured from non-renewable coal or petroleum along with a secondary thermal or chemical activation. GG can be mined from natural deposits or synthetically manufactured through the thermal treatment of carbon based materials. Such feedstock extraction and manufacturing methods for industrial GAC and GG production are energy intensive and result in the release of environmental pollutants, including CO₂ and other greenhouse.

In the context of developing cost-effective and environmentally friendly electrode material for MFCs, biomass-derived black carbon (biochar) could be a promising option. Biochar is generally a byproduct of thermal decomposition of waste biomass and has been widely used as an agricultural amendment to improve soil fertility. The use of biochar has also gained great attention as a carbon sequestration technology (Lehmann, 2007). Because biochar is generally produced from locally available bio-waste, such as agricultural and forestry residues, costs associated with feedstock purchasing, extraction and transportation are greatly reduced. In return, biochar is a more cost competitive option with prices ranging from 51 to 381 US\$ ton⁻¹ (Meyer et al., 2011), nearly ten times less than GAC and GG. There have been several recent studies demonstrating the feasibility of using waste biomass, such as aerobic sludge (Yuan et al., 2013), cardboard (Chen et al., 2012b), and crop residue (Chen et al., 2012a), as feedstock for the production of electrodes for MFCs. Such renewable resources greatly expanded the material availability, but most studies still use external energy to reach the high temperatures needed for carbonization and do not employ common manufacturing methods such as gasification, which has been widely used for biochar manufacturing and greatly reduces the final material cost. There is also little information on the characteristics of the electrodes and how they compared with other popular materials, and no information on economical and life cycle benefits of these new materials. Such information is very important as the properties of biomass based electrodes can be different with different feedstock sources and manufacturing procedures, and the main benefits of them may come from the economic and environmental aspects rather than performance.

In this study, we manufactured two different biochars for MFCs and compared their performances to GAC and GG as the anode materials. The biochars were made from compressed milling residue (BCp) and forestry residue (BCc), representing high lignin ratio waste biomass harvested from beetle-killed pine trees, using a high temperature gasification process and little external energy.

Performance and material characteristics were comprehensively investigated through electrochemical and statistical analyses, in terms of power production, resistivity, and total surface area. We also provide in this study the information for the significant economic and environmental benefits of using biochar electrodes compared to coal or petroleum based electrode materials.

2. Experimental

2.1. Electrode material characterization and manufacturing process

The main physical characteristics and costs of the four anode materials used in this study are shown in Table 1 and 2, and their natural and SEM images are shown in Fig. S1 and S2 (in Supplementary Material), respectively. The GAC was purchased from Grainger, and was manufactured from coal using industrial standard methods. GG were purchased from Graphite Sales, Inc. (Nova, OH, USA). GG material is comprised of 100% synthetic graphite made from petroleum coke. BCc and BCp were both manufactured using a custom made top-lit up-draft biomass gasifier with external fan, as described by Kearns (2012). Biomass was carbonized using a HHT of 1000 °C, residence time of 1 h., and a ramp rate of 16 °C min⁻¹ and temperature was measured using a programmable thermocouple. The BCp feedstock was compressed lodgepole pine sawdust pellets from milling residue and the BCc feedstock was lodgepole pinewood chips collected from local forestry operation.

2.2. MFC construction and operation

MFCs were constructed using two polycarbonate cube-shaped blocks separated by a cation exchange membrane (38 cm², CMI-7000, Membrane International, NJ, USA). A 37 cm diameter hole was drilled at the center of each block forming the internal anode and cathode (Wang et al., 2011a). Plain carbon cloth (38 cm², Fuel Cell Earth) was used as the common cathode material for all reactors. Each electrode material (GAC, GG, BCp or BCc) was packed into one side of anode chamber to a volume of 75 cm³ and held by a plastic mesh to tighten packing. An embedded titanium wire was used as a current collector (Wang et al., 2012). The total empty volumes were 150 and 200 ml for cathode chamber and anode chamber, respectively. MFCs were inoculated using anaerobic

Table 1
Physical and electrochemical characteristics and cost of each electrode material.

Anode material	Particle size (mm ³)	Surface resistance (Ω mm ⁻¹)	Average pore diameter (Å)	BET (cm ² g ⁻¹)	Total BET (m ²)	Material cost	
						(US\$ ton ⁻¹) ^a	US\$ m ⁻² (BET)
GAC	26–36	8 ± 2	26.8	1247.8	3.68	800–2500	1.32E-03
GG	350–450	0.4 ± 0.5	71	0.44	0.002	500–800	1.48
BCp	60–74	6 ± 1	37.6	428.6	0.52	51–381	5.04E-04
BCc	160–700	3 ± 1	29.4	470	0.32	51–381	4.60E-04

^a Material costs were determined from Meyer et al., 2011, <http://www.alibaba.com>, and personal communications with retailers.

Table 2
Summary of MFC performance and price comparison.

Anode material	Maximum power density		Total anode surface area (m ²)	Ohmic resistance (Ω)	CE (%)	Cost of power (US\$ W ⁻¹) ^b
	mW m ⁻²	W m ⁻³				
GAC	674 ± 10	7.32 ± 10	3.68	34 ± 0.9	47 ± 0.7	402.80
GG	566 ± 5	6.15 ± 5	0.002	24 ± 0.6	35 ± 0.1	392.62
BCp	532 ± 18	5.78 ± 18	0.52	34 ± 0.3	41 ± 0.4	17.27
BCc	457 ± 20	4.97 ± 20	0.32	29 ± 0.7	43 ± 0.1	35.79

^b Cost of power produced was calculated by dividing the electrode material cost per reactor by the maximum power density.

sludge from Longmont Wastewater Treatment Plant (Longmont, CO, USA). The anolyte growth medium contained 1.25 g of CH_3COONa , 0.31 g of NH_4Cl , 0.13 g of KCl , 3.32 g of $\text{NaH}_2\text{PO}_4 \cdot 2\text{H}_2\text{O}$, 10.32 g of $\text{Na}_2\text{HPO}_4 \cdot 12\text{H}_2\text{O}$, 12.5 mL of mineral solution, and 5 mL of vitamin solution per liter (Ren et al., 2007). The catholyte was 0.5 mM potassium ferricyanide solution dissolved in 50 mM phosphate buffer, which aimed to provide a stable cathode potential and minimize cathode limitation on system comparison. Each MFC was operated in fed-batch mode under a 400 Ω external resistor. When voltage dropped below 20 mV, both anolyte and catholyte were replaced with fresh media. All the tests were conducted at room temperature and repeated at least three times.

2.3. Physical, electrochemical, and statistical analyses

The surface resistance measurements were determined by randomly selecting 35 electrode samples and measuring the ohmic resistance across a 4 mm distance with a programmable multimeter. T-distribution was used to calculate confidence intervals. The cell voltages (E , volt) and electrode potentials for each MFC were measured continuously using a data acquisition system (Keithley Instrument, OH) every 66 s. Polarization curves were obtained by varying external resistances from 50,000 to 30 Ω with each resistor stabilized for 30 min (Ren et al., 2011). The anode potential and cathode potential were measured against an Ag/AgCl reference electrode (RE-5B, Bioanalysis) inserted in the anode chamber and cathode chamber, respectively (Luo et al., 2012). During acclimation and fed-batch operation cycles, circuits were connected under a fixed load (R_e , ohm) of 400 Ω . Current (I , amp) was calculated according to $I = E/R_e$. Power (P , Watt) was calculated according to $P = EI$. Current density and power density were normalized by cathode projected surface area of 38 cm^2 . Electrochemical impedance spectroscopy (EIS) was conducted by a potentiostat (PC4/3000, Gamry Instruments, NJ, USA) to determine total internal resistance using the anode as the working electrode, and the cathode as the counter electrode and reference electrode (Wang et al., 2011b). The electrochemical experiments performed on each material and corresponding reactor were conducted after two months of continuous operation and carried out in triplicates in order to determine the standard deviation.

Brunauer–Emmett–Teller (BET) method that uses a five-point N_2 gas adsorption technique (ASAP 2020; Micromeritics, Norcross, GA) was used to measure the specific surface area and pore size distribution of the electrode materials. Average pore size and pore size distribution was determined from desorption of N_2 according to the method developed by Barrett, Joyner, and Halenda (Elliott et al., 1951).

3. Results and discussion

3.1. Power production and columbic efficiency

Measuring the maximum power output and columbic efficiency (CE) are two common methods used to evaluate the performance of MFCs. The CEs and maximum power densities from MFCs equipped with the four different anode materials (BCp, BCc, GAC and GG) are summarized in Table 1 and Fig. 1, with power densities normalized by cathode projected surface area. Fig. 2 demonstrates the power output profiles after 1 month of fed-batch operations. Results showed that the GAC anode achieved the highest CE at around 47%, and GG had the lowest CE at 35%. The CEs from BCc and BCp were comparable at 41–43%. GAC had the highest power density of $674 \pm 10 \text{ mW m}^{-2}$, followed by GG with $566 \pm 5 \text{ mW m}^{-2}$, BCp with $532 \pm 18 \text{ mW m}^{-2}$ and BCc with $457 \pm 20 \text{ mW m}^{-2}$.

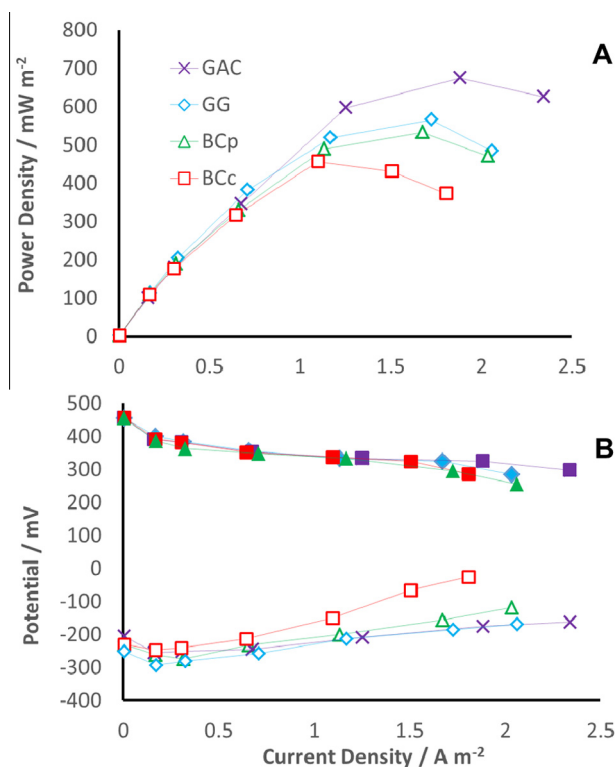


Fig. 1. (A) Power density curve normalized by cathode projected area and (B) electrode potentials (cathode, filled symbols; anode, open symbols) versus Ag/AgCl reference electrode as a function of current density in MFCs packed with GAC, GG, BCp and BCc.

Cathode potentials for all four reactors were comparable as designed, because ferricyanide cathode was used to normalize the cathode potential and is illustrated in Fig. 1. The anode potential of BCc increased to around 0.0 mV at 1.8 A m^{-2} , which resulted in lower power output. It was hypothesized that the difference in power densities can be attributed to the difference in material surface area density, particle size, and system internal resistance, which will be explained in more detail in the following sections. It must be noted that the power density differences are not an intrinsic value of the biochar material, and it could be manipulated through variations in feedstock selection and manufacturing. As research in this field matures, biochar electrodes could be manufactured in such a way to mimic the beneficial properties of both GAC and GG, while maintaining its integrity as a low-cost electrode material.

3.2. Surface characteristics of electrode materials

High surface area and low resistance are two fundamental characteristics to define good electrode materials and affect MFC power output performance. While this section discusses the characteristics of surface area and porosity of the four materials, the next section elucidates the effects of resistance. Table 1 and Fig. 3 show the average pore diameter of the materials using the Brunauer–Emmett–Teller (BET) test. Results show that the GAC has the highest BET surface area of $1247.8 \text{ cm}^2 \text{ g}^{-1}$, followed by BCp and BCc with $469.9 \text{ m}^2 \text{ g}^{-1}$ and $428.6 \text{ cm}^2 \text{ g}^{-1}$ respectively. GG had the lowest BET surface area of $0.44 \text{ cm}^2 \text{ g}^{-1}$. The average pore size for GAC is 20–30 Å, while the BCp and BCc samples had an average of 30–40 Å. While the high surface area can explain why GAC obtained a higher power density due to the increased substrate availability and microbial attachment on the electrode, it is hard to directly

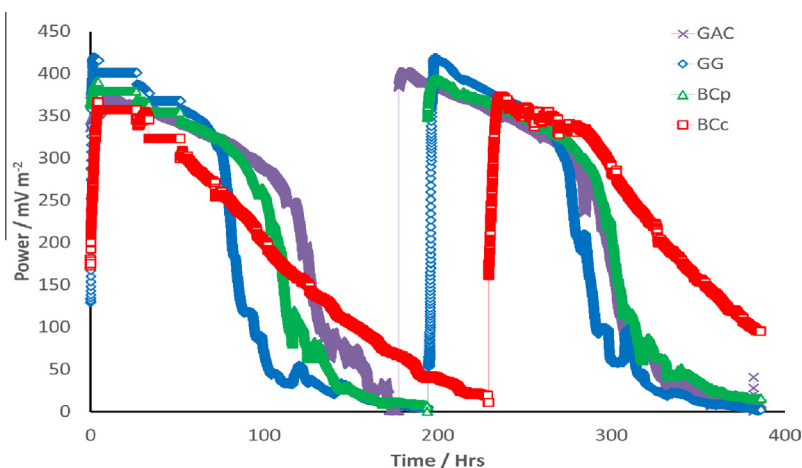


Fig. 2. Power production during consecutive fed-batch experiments after 1 month of continuous operation.

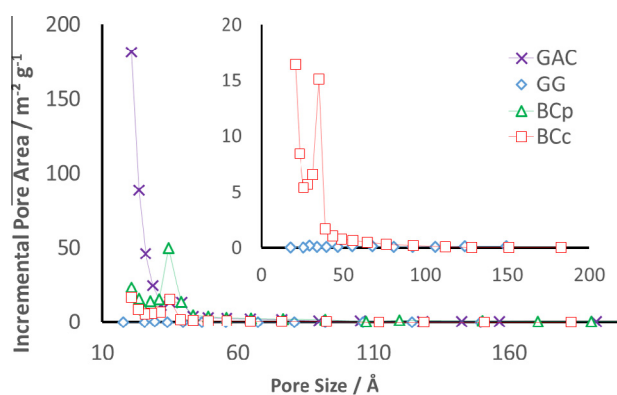


Fig. 3. Incremental pore area and pore size distribution of the four electrode materials.

correlate the low surface area of graphite with low power output. As shown in Fig. 1, graphite electrode had a higher power density than the biochar electrodes despite its low surface area, presumably due to its higher conductivity.

The higher surface area of GAC is primarily caused by the secondary activation process carried out during manufacturing, in which reactive components of the feedstock material are removed by the use of oxidizing agents, such as steam or carbon dioxide (Summers et al., 2010). The wood derived biochar samples used in this study and GGs did not undergo this activation step, but the forced air updraft gasification pyrolysis process used to manufacture both biochar samples reliably produces chars with BET SA 400–500 m² g⁻¹. The gasification pyrolysis process reached a highest treatment temperature (HTT) of 1000 °C with a heating rate of 16.6 °C min⁻¹, in the process lignocellulosic materials are converted to a highly condensed aromatic char composed of carbon. The HTT and heating rate are reported to significantly influence the physical structure of the feedstock material during carbonization. For example, studies showed that higher surface area was achieved at temperatures between 750 and 850 °C (Mochidzuki et al., 2003), but sintering and deformation may occur at higher temperatures (Lua and Guo, 1998). Brown et al. (2006) provides evidence that higher surface area is achieved with higher heating rate, because such process leads to cracking at low temperatures by unevenly heating the feedstock material and these cracks provided access to more internal pores. Furthermore, the transition from low-density amorphous carbon to high-density crystallites

leads to the formation of nanopores ($d < 2$ nm) (Kercher and Nagle, 2003).

Along with HTT and heating rate, the inherent porosity and structure of the feedstock material can also affect the internal surface area. Several studies showed that biomass based chars possess high surface area and adsorption capacity and could be cheaper surrogates for GAC type electrode materials (Brown et al., 2006). In many cases, the archetypal cellular structure of the parent feedstock material is identifiable in chars derived from botanical origin, resulting in a honeycomb-like structure that significantly contributes to the majority of macroporosity. Scanning electron microscope (SEM) photos can be seen in Fig. S2 and the difference in surface morphology can clearly be seen. Both biochar samples have larger pores and the parent plant structure of BCc is easily identified. These macropores act as conduits to smaller micropores and increase the overall internal surface area. The macropores could also facilitate the adsorption of larger organic molecules, compared to micropores, and could be used to aid in wastewater treatment.

Although there is a growing body of literature on the effects of manufacturing methods on the chemical and physical properties of biochar and other biomass based absorbent materials, there is little understanding of how surface area density and pore size distribution affect microbial growth, abundance, and adhesion. The increased physiochemical adsorption of substrates due to increased surface area is believed to boost microbial electrochemical activities, but it will unlikely change the approach exoelectrogens used for extracellular electron transfer. Some of the larger pores can be accessible for microbial adhesion, and smaller micropores may contribute to the increased conductivity due to increased specific surface area for electron transfer. This study highlights that microporosity is important for increased power density, but additional research is needed to refine the manufacturing of biochar in order to increase the desired characteristics as MFC electrodes while maintaining economic benefits.

3.3. Resistance characteristics of electrode materials

Similar to surface area, internal resistance (R_i) is one of the major factors affecting power density in MFCs. The total R_i can be separated into three components, activation, ohmic and concentration resistances (Logan et al., 2006). The activation resistance occurs when electrons are transferred to or from a compound, primarily during oxidation/reduction reactions and relates to the anode catalytic efficiency. The ohmic resistance occurs when electrons and ions transfer through the solution, electrodes, and separators. The concentration resistance is due to the rate of chemical mass

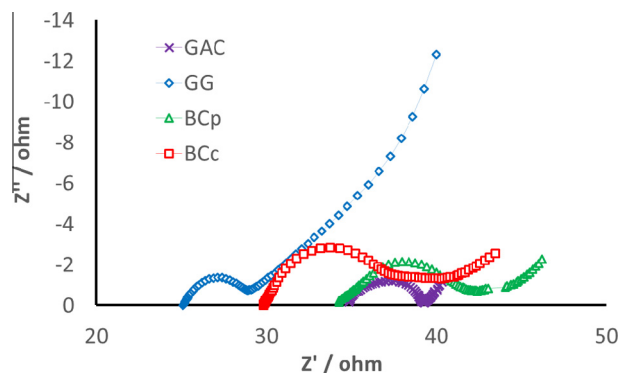


Fig. 4. Nyquist plots showing system resistances of the reactors with four different materials.

transport to or from the electrode. Fig. 4 shows the electrochemical impedance spectroscopy (EIS) findings demonstrating the differences in internal resistances of the four materials. The Nyquist graph shows that GG has the lowest ohmic resistance of $24 \pm 0.6 \Omega$, followed by BCc with $29 \pm 0.7 \Omega$, BCp with $34 \pm 0.3 \Omega$, and GAC with $34 \pm 0.9 \Omega$ (Table 2). This shows a similar trend as material surface resistance measured by a multimeter (Table 1), where GG has the lowest surface resistance of $0.4 \pm 0.5 \Omega \text{ mm}^{-1}$, much lower than the biochar materials and GAC. However, when counting the total R_i of each material, GG and GAC had a similar total resistance of 39 ± 9 and $40 \pm 3 \Omega$ respectively, while BCp and BCc had a slightly higher R_i of 46 ± 2 and $43 \pm 3 \Omega$, respectively. The ohmic resistance is responsible for nearly 86%, 62%, 74% and 68% of the total R_i in the GAC, GG, BCp, and BCc reactors, respectively, but it cannot explain entirely the difference in the observed power densities. On the other hand, the activation resistance for BCp and BCc was 7 ± 0.9 and $8 \pm 0.1 \Omega$ respectively, almost doubled than GAC with $4 \pm 0.6 \Omega$ and GG with $4 \pm 0.2 \Omega$ (Fig. 4). Higher activation resistance is thought to be attributed to the lack of rigorous surface preparation as compared to the commercial GAC and GG products. The higher activation resistance of the biochar electrodes partially explains the relatively lower power output, despite their lower ohmic resistance compared to GAC.

3.4. Economic and environmental benefits of using biochar as electrode materials

Biochar is traditionally manufactured from renewable biomass feedstock such as forestry, milling, and agriculture residue, along with yard clippings and construction waste (Lehmann & Joseph, 2009). The utilization of locally available waste biomass, with little to no commercial value, greatly reduces the costs associated with purchasing and transportation. Using biomass feedstock also significantly reduces harmful emissions of mercury and sulfur and the resulting biochar fixes and stores the atmospheric carbon. For the purpose of this study we used waste beetle-killed lodgepole pine wood chips collected from a forestry site and compressed milling residue pellets, representing a locally available waste biomass feedstock. The only costs associated with the wood based electrodes were due to transportation of the forestry residue and the milling residue pellets were purchased locally for 5 US\$ per 20 lb^{-1} bag. Utilizing a locally available waste product allowed us to avoid the high costs associated with feedstock purchasing and greatly reduced the cost of manufacturing. Furthermore, there was no need for pretreatment of the material and little external energy was required during manufacturing. Factoring the purchasing of feedstock, transportation, manufacturing and an additional 15% for labor, we estimate the cost of manufacturing the biochar

electrodes to be around $0.46 \text{ US\$ lb}^{-1}$. This is 90% less than the GAC used in this experiment which was purchased for around $5 \text{ US\$ lb}^{-1}$ and 60% less than the GG used in this experiment which was purchased for around $1 \text{ US\$ lb}^{-1}$. When power density and material costs were taken into consideration based on previous MFC studies, the biochar electrodes (BCp and BCc) can be an order of magnitude more cost effective ($17\text{--}35 \text{ US\$ W}^{-1}$) than GAC and GG ($393\text{--}403 \text{ US\$ W}^{-1}$) and is outlined in Table 2.

In addition to the benefits of low cost and renewable feedstock, the manufacturing method also contributes significantly to the environmental impact, final characteristics and cost of biochar electrodes. Biochar is commonly manufactured from the pyrolysis or gasification of biomass. In this study we used a top-lit-up-draft gasification furnace that generates the high heat ($>1000 \text{ }^\circ\text{C}$) required for carbonization by combusting the syngas released during volatilization of the feedstock. This is an exothermic process that requires little external energy. In contrast, the manufacturing of GAC, GG, and other electrode materials commonly uses external energy to control the heating rate and perform a thermal activation step, which raises the overhead costs of manufacturing and depending on the energy source, results in additional release of environmental pollutants.

Along with energy production, land application of biochar has shown additional carbon offsets, improved soil fertility and cost reductions. The benefits of biochar addition to agricultural soils includes improved water and nutrient retention, increase crop yield, suppressed N_2O emissions, reduce fertilizer requirements, and increased soil organic carbon content (Sohi et al., 2010). Because of the beneficial effects of biochar addition to soil, we suggest that the spent biochar electrode could be composted and used as a soil application after sterilization, which could have similar, if not increased, beneficial effects on agricultural production. When used as an electrode material in MFCs treating wastewater, valuable micronutrients could be adsorbed and slowly released in agricultural field after application. Biochar made from forest residue has been shown to be an effective surrogate for activated carbon having similar adsorption capabilities (Zhang et al., 2004). Biochar materials have also shown to efficiently adsorb phosphorus and other nutrients from aqueous solution (Yao et al., 2011). However, further research is required to verify this and to determine if any problematic compounds or pathogens would accumulate in the agroecosystem. If sufficient evidence is collected to demonstrate the beneficial use of spent biochar electrodes as agricultural amendments, it could significantly offset the cost of MFC construction and operation.

Despite the life-cycle and cost benefits of using biochar as MFC electrode materials, additional research is needed to refine the production method and assess the full life-cycle benefits in terms of feedstock selection, manufacturing, and land application. Great care should be taken to select feedstock material with little economic value, while maximizing the energy output during manufacturing. Not every biochar sample is the same, in order for biochar to be used as electrode materials, manufacturing parameters should be set to produce chars with high surface area and conductivity to increase their performance in MFCs. In general, higher carbonization temperatures lead to increased surface area, electrical conductivity, recalcitrance, and tensile strength (Downie et al., 2009). This is due to volatilization of the liable fraction of biomass, increased fixed carbon ratio and transformation from low-density disordered carbon to the formation of high-density aromatic crystalline carbon structures (Keiluweit et al., 2010). It is clear that the aromatic structure of biochar is what makes extremely environmentally stable and has been suggested to remain chemically unchanged over millennial (Nguyen et al., 2010). Feedstock also plays a vital role in the final characteristics of biochar (Keiluweit et al., 2010), in general woody biomass with high lignin to cellulose

ratio should be selected over herbaceous biomass to increase yield, electrical conductivity, and stability at lower temperatures (Liu et al., 2013). This can be attributed to the thermal stability and lower electrical resistivity of lignin compared to cellulose (Kumar and Gupta, 1993). The feasibility, risk and benefits, along with carbon sequestration potential during land application of spent biochar electrodes should also be investigated.

4. Conclusion

Biochar materials, made from lodgepole pine wood chips (BCc) and compressed milling residue (BCp), were tested as electrode materials in microbial fuel cells. Both materials showed satisfactory power density comparable to GG and GAC electrodes, but biochar costs significantly less than GAC or GG due to its feedstock and one-step manufacturing process. Biochar carries environmental benefits such as biowaste feedstock, energy positive manufacturing, carbon sequestration potential, and land application as agricultural amendment, but further research is needed to optimize the manufacturing method of biochar electrode production and increase its performance.

Acknowledgements

This work was supported by the Bill & Melinda Gates Foundation's Grand Challenges Explorations Grant OPP1043362 and the Office of Naval Research University Laboratory Initiative Grant N000141210293.

Appendix A. Supplementary data

Supplementary data associated with this article can be found, in the online version, at <http://dx.doi.org/10.1016/j.biortech.2014.01.058>.

References

- Brown, R.A., Kercher, A.K., Nguyen, T.H., Nagle, D.C., Ball, W.P., 2006. Production and characterization of synthetic wood chars for use as surrogates for natural sorbents. *Org. Geochem.* 37, 321–333.
- Chen, S., He, G., Hu, X., Xie, M., Wang, S., Zeng, D., Hou, H., Schröder, U., 2012a. A three-dimensionally ordered macroporous carbon derived from a natural resource as anode for microbial bioelectrochemical systems. *ChemSusChem* 5, 1059–1063.
- Chen, S., He, G., Liu, Q., Harnisch, F., Zhou, Y., Chen, Y., Hanif, M., Wang, S., Peng, X., Hou, H., Schröder, U., 2012b. Layered corrugated electrode macrostructures boost microbial bioelectrocatalysis. *Energy Environ. Sci.* 5, 9769.
- Downie, A., Crosky, A., Munroe, P., 2009. Physical properties of biochar. In: *Biochar for Environmental Management: Science and Technology*. Earthscan.
- Elliott, P.B., Leslie, G.J., Paul, P.H., 1951. The determination of pore volume and area distributions in porous substances. *J. Am. Chem. Soc.* (1896).
- Huggins, T., Fallgren, P., Jin, S., Ren, Z., 2013. Energy and performance comparison of microbial fuel cell and conventional aeration treating of wastewater. *J. Microb. Biochem. Technol.*, S6–2.
- Kearns, J., 2012. Sustainable decentralized water treatment for rural and developing communities using locally generated biochar adsorbents (spotlight). *Water Cond. Purif.*, 7–12.
- Keiluweit, M., Nico, P.S., Johnson, M.G., Kleber, M., 2010. Dynamic molecular structure of plant biomass-derived black carbon (biochar). *Environ. Sci. Technol.* 44, 1247–1253.
- Kercher, A.K., Nagle, D.C., 2003. Microstructural evolution during charcoal carbonization by X-ray diffraction analysis. *Carbon* 41, 15–27.
- Kumar, M., Gupta, R., 1993. Electrical resistivity of *Acacia* and *Eucalyptus* wood chars. *J. Mater. Sci.* 28, 440–444.
- Lehmann, J., 2007. A handful of carbon. *Nature* 447, 143–144.
- Lehmann, J., Joseph, S. (Eds.), 2009. *Biochar for Environmental Management: Science and Technology*. Earthscan.
- Liu, Z., Demisie, W., Zhang, M., 2013. Simulated degradation of biochar and its potential environmental implications. *Environ. Pollut.* 179, 146–152.
- Logan, B.E., 2008. *Microbial fuel cells*. Wiley (Wiley.com).
- Logan, B.E., Hamelers, B., Rozendal, R., Schröder, U., Keller, J., Freguia, S., Aelterman, P., Verstraete, W., Rabaey, K., 2006. Microbial fuel cells: methodology and technology. *Environ. Sci. Technol.* 40, 5181–5192.
- Lua, A.C., Guo, J., 1998. Preparation and characterization of chars from oil palm waste. *Carbon* 36, 1663–1670.
- Luo, H., Xu, P., Jenkins, P.E., Ren, Z., 2012. Long-term performance and characterization of microbial desalination cells in treating domestic wastewater. *Bioresour. Technol.* 120, 187–193.
- Meyer, S., Glaser, B., Quicker, P., 2011. Technical, economical, and climate-related aspects of biochar production technologies: a literature review. *Environ. Sci. Technol.* 45, 9473–9483.
- Mochidzuki, K., Soutiric, F., Tadokoro, K., Antal, M.J., Tóth, M., Zelei, B., Várhegyi, G., 2003. Electrical and physical properties of carbonized charcoals. *Ind. Eng. Chem. Res.* 42, 5140–5151.
- Nguyen, B.T., Lehmann, J., Hockaday, W.C., Joseph, S., Masiello, C.A., 2010. Temperature sensitivity of black carbon decomposition and oxidation. *Environ. Sci. Technol.* 44, 3324–3331.
- Rabaey, K., Bützler, S., Brown, S., Keller, J., Rozendal, R.A., 2010. High current generation coupled to caustic production using a lamellar bioelectrochemical system. *Environ. Sci. Technol.* 44, 4315–4321.
- Ren, Z., Ward, T.E., Regan, J.M., 2007. Electricity production from cellulose in a microbial fuel cell using a defined binary culture. *Environ. Sci. Technol.* 41, 4781–4786.
- Ren, Z., Yan, H., Wang, W., Mench, M.M., Regan, J.M., 2011. Characterization of Microbial Fuel Cells at Microbially and Electrochemically Meaningful Time scales. *Environ. Sci. Technol.* 45, 2435–2441.
- Rozendal, R.A., Leone, E., Keller, J., Rabaey, K., 2009. Efficient hydrogen peroxide generation from organic matter in a bioelectrochemical system. *Electrochem. Commun.* 11, 1752–1755.
- Sohi, S.P., Krull, E., Lopez-Capel, E., Bol, R., 2010. A review of biochar and its use and function in soil. In: Donald, L.S. (Ed.), *Advances in Agronomy*, Vol. 105. Academic Press, pp. 47–82 (Chapter 2).
- Summers, R., Knappe, D., Snoeyink, V., 2011. Adsorption of organic compounds by activated carbon. In: *Water Quality & Treatment: A Handbook on Drinking Water*. McGraw-Hill.
- Wang, H., Ren, Z.J., 2013. A comprehensive review of microbial electrochemical systems as a platform technology. *Biotechnol. Adv.* 31, 1796–1807.
- Wang, H., Davidson, M., Zuo, Y., Ren, Z., 2011. Recycled tire crumb rubber anodes for sustainable power production in microbial fuel cells. *J. Power Sources* 196, 5863–5866.
- Wang, H., Wu, Z., Plaseied, A., Jenkins, P., Simpson, L., Engtrakul, C., Ren, Z., 2011. Carbon nanotube modified air-cathodes for electricity production in microbial fuel cells. *J. Power Sources* 196, 7465–7469.
- Wang, H., Park, J., Ren, Z., 2012. Active energy harvesting from microbial fuel cells at the maximum power point without using resistors. *Environ. Sci. Technol.* 2012 (46), 5247–5252.
- Wei, J., Liang, P., Huang, X., 2011. Recent progress in electrodes for microbial fuel cells. *Bioresour. Technol.* 102, 9335–9344.
- Yao, Y., Gao, B., Inyang, M., Zimmerman, A.R., Cao, X., Pullammanappallil, P., Yang, L., 2011. Removal of phosphate from aqueous solution by biochar derived from anaerobically digested sugar beet tailings. *J. Hazard. Mater.* 190, 501–507.
- Yuan, Y., Yuan, T., Wang, D., Tang, J., Zhou, S., 2013. Sewage sludge biochar as an efficient catalyst for oxygen reduction reaction in a microbial fuel cell. *Bioresour. Technol.* 144, 115–120.
- Zhang, T., Walawender, W.P., Fan, L.T., Fan, M., Daugaard, D., Brown, R.C., 2004. Preparation of activated carbon from forest and agricultural residues through CO₂ activation. *Chem. Eng. J.* 105, 53–59.